



# Coevolving spreading dynamics of negative information and epidemic on multiplex networks

Jiaxing Chen · Ying Liu · Jing Yue ·  
Xi Duan · Ming Tang

Received: 21 January 2022 / Accepted: 4 August 2022 / Published online: 23 August 2022  
© The Author(s), under exclusive licence to Springer Nature B.V. 2022

**Abstract** The widespread dissemination of negative information on vaccine may arise people's concern on the safety of vaccine and increase their hesitancy in vaccination, which can seriously impede the progress of epidemic control. Existing works on information-epidemic coupled dynamics focus on the suppression effects of information on epidemic. Here we propose a negative information and epidemic coupled propagation model on two-layer multiplex networks to study the effects of negative information of vaccination on epidemic spreading, where the negative information propagates on the virtual communication layer and the disease spreads on the physical contact layer. In our model, an individual getting an adverse event after

vaccination will spread negative information and an individual affected by the negative information will reduce his/her willingness to get vaccinated and spread the negative information. By using the microscopic Markov chain method, we analytically predict the epidemic threshold and final infection density, which agree well with simulation results. We find that the spread of negative information leads to a lower epidemic outbreak threshold and a higher final infection density. However, the individuals' vaccination activities, but not the negative information spreading, has a leading impact on epidemic spreading. Only when the individuals obviously reduce their vaccination willingness due to negative information, the negative information can impact the epidemic spreading significantly.

J. Chen · Y. Liu (✉) · J. Yue  
School of Computer Science, Southwest Petroleum  
University, Chengdu 610500, China  
e-mail: shinningliu@163.com

X. Duan  
School of Science, Southwest Petroleum University,  
Chengdu 610500, China

J. Chen  
Tianjin Key Lab of Intelligence Computing and Novel  
Software Technology, Tianjin University of Technology,  
Tianjin 300384, China

M. Tang  
School of Physics and Electronic Science, East China  
Normal University, Shanghai 200241, China

M. Tang  
Shanghai Key Laboratory of Multidimensional Information  
Processing, East China Normal University, Shanghai 200241,  
China

**Keywords** Multiplex network · Negative information · Information-epidemic coupled dynamics · Microscopic Markov chain approach

## 1 Introduction

The human beings are fighting with epidemics for a long history, such as Dengue, Severe Acute Respiratory Syndrome (SARS), Ebola and recently prevalent COVID-19 infectious disease [1–3]. Mathematical model lies at the core of understanding the spreading of infectious disease. Some basic models such as susceptible-infected-susceptible (SIS) and susceptible-infected-recovered (SIR) models are pro-

posed to describe the dynamical evolution of the contagion progresses in the population [4]. Researches on the epidemic models greatly improve our understanding of epidemic spreading and help to control epidemics [5].

Nowadays, with the rapid development of information technology, people are quite convenient to exchange information with others through different kinds of communication channels, such as the mobile phone, email and online social platforms of Twitter, Facebook, WeChat, etc. When an epidemic breaks out in one or more locations in the world, information on epidemic transmits and stimulates risk awareness of people, which helps to suppress the spreading of epidemic [6]. The interrelated dynamics of information diffusion and epidemic spreading are modeled and analyzed as the asymmetrically interacting processes on multiplex networks [7–12]. A multiplex network consists of several layers representing different types of interactions between nodes, where the actors in different layers are the same. In a typical awareness-epidemic coevolution model on two-layer multiplex networks, the epidemic spreading is described by the SIS propagation dynamics on the physical contact network, and the diffusion of awareness arisen by information is described by the unawareness–awareness–unawareness (UAU) propagation dynamics on the virtual communication layer [7]. Some non-trivial phenomena were discovered that are substantially different from the independent spreading dynamics in single networks. For example, the critical point of the asymmetrically coupled spreading process depends on the topology of the communication network and the dynamics of information dissemination [7], while the mass media makes the critical point disappear [8]. The information outbreak can be triggered by its own spreading dynamics or by a disease outbreak, and there is an optimal information transmission rate at which the information remarkably suppresses the disease spreading [13]. Moreover, some works considered the timescales of information diffusion and disease spreading, and it was found that an optimal relative timescale may reduce the incidence of epidemics [14, 15]. Within the framework, a plenty of information-disease coupled spreading models were proposed enriching our understanding of the coevolution dynamics [16–21].

In the real online community, there are not only official and authentic information on the severity and danger of epidemics, but also a great deal of unreli-

able information, misinformation or even fake news [22, 23]. For example in the early stage of COVID-19, the public is exposed to infodemic, the rapid and far-reaching spread of unreliable information, which is found to precede the rise of infections [24]. As the number of infections rises, science-based information quickly becomes dominant, which helps to suppress the epidemic [24, 25]. One of the negative effects of unreliable information in health-related fields is that it impacts public confidence in vaccination and causes vaccination hesitancy. Because people are extremely sensitive to the importance, safety and effectiveness of vaccines [26], individuals affected by negative information on vaccine safety may become hesitant to receive vaccination. The collective outcome of individuals' decisions of not vaccinating reduces the coverage of vaccine, which does harm to the suppression of a pandemic or makes some epidemics that could have been prevented by vaccines break out again [27, 28]. In a survey, 6.2 percentage of volunteers in the UK and 6.4 percentage of volunteers in the USA expressed varying degrees of unwillingness to vaccination, after they watched negative information about the COVID-19 vaccine [29]. It was also found that a small adverse event of vaccine may cause a steep decline in vaccination coverage [30].

At present, a lot of works have analyzed the impact of the dissemination of negative information on vaccination and disease transmission [31, 32], but the mathematical modeling that quantitatively describes the influence of negative information of vaccination on the spreading dynamics of the epidemic is still lacking. In ref. [33], the authors worked on the coevolution of negative information on vaccine inefficiency and epidemic spreading on three-layer networks, where the susceptible-infected-susceptible (SIS) dynamics is used to describe information spreading and disease spreading, with a third layer on which the vaccination behavior spreads. In reality, there are some diseases that people retain immunity once they recover from them and cannot be infected by them again, which should be modeled as the SIR dynamics. For example, the COVID-19 epidemic is modeled as the SIR-type dynamics [3, 34]. In addition, in ref. [33] they worked on the negative information related to the inefficiency of vaccines. However, when facing with new or urgent vaccines, the safety of vaccines is more sensitive for people to make their decisions to receive vaccination or not.

In this paper, we propose a coevolving spreading model of negative information and epidemic disease. We construct a multiplex network composed of a virtual communication network and a physical contact network, where the negative information on vaccine safety and the epidemic spread, respectively. Nodes on the contact layer get vaccinated, and a small fraction of them may have adverse events, which is the source of negative information. The negative information spreads on the communication network and nodes affected by negative information will reduce their willingness to vaccinate and spread negative information. By using the microscopic Markov chain approach (MMCA), we calculate the epidemic threshold and the final infection density, which agree well with the simulation results. Large simulation results indicate that the propagation of negative information reduces the epidemic threshold and increases the final infection size. Compared with negative information, people's hesitancy in vaccination has a more significant effects on the epidemic spreading.

The rest of the paper is organized as follows: In Sect. 2, the negative information-epidemic coupled propagation model is introduced. In Sect. 3, we use the microscopic Markov chain approach to calculate the epidemic threshold, final infection size and vaccination coverage. In Sect. 4, we compare the MMCA predictions with the numerical simulation results and analyze the impact of parameters. Finally in Sect. 5, we make conclusion and discussion.

## 2 The model

We define a negative information-epidemic coupled propagation model on the multiplex network to describe the coevolving dynamics of information and disease. Figure 1 illustrates the model and the state transitions of nodes. The network consists of a virtual communication layer and a physical contact layer, where the negative information and disease spread, respectively, as shown in Fig. 1a. In the communication layer, the information spreads in an unaware-aware-recovered (UAR) dynamics, as shown in Fig. 1b. An unaware ( $U$ ) node can be informed by the aware ( $A$ ) node at the information transmission rate  $\beta_A$ . The nodes of  $A^+$  state are those who have vaccinated and got adverse events. Because they undergo the side effects themselves, the negative information transmitted by them is more con-

vincing. Thus, the information transmission rate of  $A^+$  nodes is  $\beta_A^+ = c\beta_A$ , where  $c$  is the information transmission enhancement coefficient. If  $\beta_A^+$  is greater than 1, we take it as 1. Both the  $A$  nodes and  $A^+$  nodes recover to the  $R_A$  state at rate  $\mu_A$ , representing that they will not transmit information any more. There is also a  $R_U$  state, which represents that a node has vaccinated and has not gotten adverse event. These nodes do not transmit negative information on the communication layer. In the physical contact layer as shown in Fig. 1c, the classical susceptible-infected-removed-vaccinated (SIRV) model is used, where an infected ( $I$ ) node transmits disease to each of its susceptible ( $S$ ) neighbors at rate  $\beta_B$  and then becomes removed ( $R$ ) at rate  $\mu_B$ . The  $S$  nodes becomes vaccinated at rate  $m^U$  or  $m^A$ , where its counterpart in the communication layer is in  $U$  state or  $A$  state, respectively, and  $m^A = \gamma m^U$ . Here  $\gamma$  is the vaccination attenuation factor and  $0 \leq \gamma \leq 1$ .

The interplay between the two layers is shown in Fig. 1 d and e. In Fig. 1d, the impact of the communication layer on the contact layer is demonstrated. For a node  $i_A$  in  $U$  state in the communication layer, its counterpart  $i_B$  in the contact layer gets vaccinated at rate  $m^U$ . If  $i_A$  is in the  $A$  state or  $R_A$  state,  $i_B$  gets vaccinated at rate  $m^A$ . This corresponds to the case that the individuals affected by the negative information reduce their willingness to take vaccine. In Fig. 1e, the impact of the contact layer on the communication layer is demonstrated. If a node  $i_B$  is infected, its counterpart  $i_A$  in the communication layer will not transmit negative information. This is based on the assumption that an infected individual has to believe the danger of epidemic. So  $i_A$  becomes  $R_U$  immediately if it is of  $U$  state, or changes to  $R_A$  if it is of  $A$  state. On the other hand, for a vaccinated node  $i_B$ , there is a probability  $\alpha_V$  that a vaccine adverse event occurs. In this case, its counterpart  $i_A$  becomes  $A^+$  if it is in  $U$  state,  $A$  state or  $R_A$  state. Otherwise with probability  $1 - \alpha_V$ , the node  $i_A$  becomes  $R_U$  or  $R_A$ .

Symbols used in this paper are listed in Table 1.

## 3 Microscopic Markov chain approach

We use the microscopic Markov chain approach (MMCA) to describe the negative information-epidemic coupled dynamics in the multiplex networks. We denote the probability that node  $i$  is in  $X$  state at time  $t$  as  $p_i^X(t)$ , where  $X \in (U, A, A^+, R_U, R_A, S, I, R, V, US, AS, A^+V, R_AV, R_UV, R_UI, R_AI, R_AS, R_AR,$

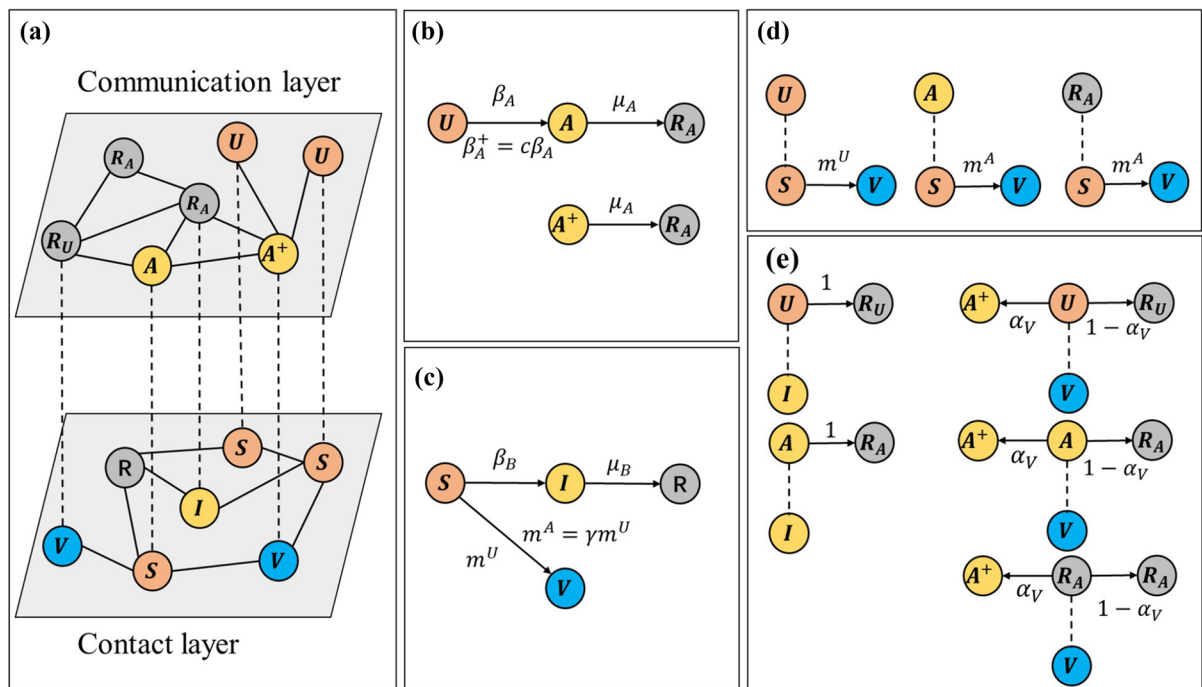


**Fig. 1** Illustration of the negative information-epidemic coupled spreading dynamics on a multiplex network. **a** The multiplex network consists of a communication layer and a physical contact layer. Each node in the communication layer has a counterpart in the contact layer and vice versa. **b** In the communication layer, a  $UAR$  dynamics is adopted. The information transmission rates for  $A$  and  $A^+$  nodes are  $\beta_A$  and  $\beta_A^+$ , respectively. The nodes of state  $A$  recover at rate  $\mu_A$ . **c** In the contact layer, the  $SIRV$  dynamics is adopted. The disease transmission rate is  $\beta_B$ , and

nodes of  $I$  state recover at rate  $\mu_B$ . **d** Under the impact of the communication layer, the nodes of  $S$  state change to  $V$  state at different rates. The  $S$  nodes in the contact layer are vaccinated with probability  $m^U$  or  $m^A$ . **e** Under the impact of the contact layer, the states of nodes in  $U$ ,  $A$  or  $R_A$  states change. The counterpart of an  $I$  node changes to  $R_U$  or  $R_A$  state. For a  $V$  state node, its counterpart changes to  $A^+$  at probability  $\alpha_V$ , corresponding to the case that an adverse event happens. Otherwise, the counterpart node changes to  $R_U$  or  $R_A$  state

**Table 1** Symbols used in the paper

Symbol	Description
$a_{ij}$	Element in the adjacency matrix of communication layer
$b_{ij}$	Element in the adjacency matrix of contact layer
$k$	Degree of node
$\beta_A$	Information transmission rate
$\beta_A^+$	Enhanced information transmission rate, $\beta_A^+ = c\beta_A$
$c$	Information transmission enhancement coefficient
$\beta_B$	Disease transmission rate
$\beta_B^c$	Epidemic threshold
$\mu_A$	Information recovery rate
$\mu_B$	Disease recovery rate
$m^U$	Basic vaccination rate
$m^A$	Attenuated vaccination rate, $m^A = \gamma m^U$
$\gamma$	Vaccination attenuation factor

**Table 1** continued

Symbol	Description
$\alpha_V$	Probability that an adverse event of vaccine occurs
$r_i(t)$	Probability of node $i$ not being informed by any neighbor at time $t$
$q_i(t)$	Probability of node $i$ not being infected by any neighbor at time $t$
$p_i^X(t)$	Probability of node $i$ being in X state at time $t$
$p_i^X$	Probability of node $i$ being in X state in the stationary state
$\rho^X$	Density of nodes in X state in the stationary state

$R_U R$ ), where the set  $(U, A, A^+, R_U, R_A)$  are states of nodes in the communication layer, the set  $(S, I, R, V)$  are states of nodes in the contact layer, and the set  $(US, AS, A^+V, R_A V, R_U V, R_U I, R_A I, R_A S, R_A R, R_U R)$  are states of nodes in the coupled dynamics. The elements in the adjacency matrices of the communication layer and the contact layer are  $a_{ij}$  and  $b_{ij}$ , respectively. On the communication layer where negative information spreads, the probability that an unaware node is not informed by any aware neighbor at time  $t$  is

$$r_i(t) = \prod_j \left[ \left( 1 - a_{ij} p_j^{A^+}(t) \beta_A^+ \right) \left( 1 - a_{ij} p_j^A(t) \beta_A \right) \right], \quad (1)$$

where  $\beta_A^+$  and  $\beta_A$  are the information transmission rates of  $A^+$  nodes and  $A$  nodes, respectively, and  $\beta_A^+ = c\beta_A$ .

On the contact layer, the probability of a susceptible node not being infected by any infected neighbor at time  $t$  is

$$q_i(t) = \prod_j \left[ 1 - b_{ij} p_j^I(t) \beta_B \right], \quad (2)$$

where  $\beta_B$  is the disease transmission rate. The transition probability trees for the states of  $US, AS, A^+V, R_A I$  and  $R_U I$  nodes are demonstrated in Fig. 2.

Then, the evolution equations of the coupled spreading dynamics can be written as:

$$p_i^{US}(t+1) = p_i^{US}(t) r_i(t) (1 - m^U) q_i(t), \quad (3)$$

$$p_i^{AS}(t+1) = p_i^{US}(t) (1 - r_i(t)) (1 - m^A) q_i(t), \quad (4)$$

$$p_i^{RAS}(t+1) = p_i^{AS}(t) (1 - m^A) q_i(t) + p_i^{RAS}(t) (1 - m^A) q_i(t), \quad (5)$$

$$p_i^{A^+V}(t+1) = p_i^{US}(t) (1 - r_i(t)) m^A \alpha_V + p_i^{US}(t) r_i(t) m^U \alpha_V + p_i^{RAS}(t) m^A \alpha_V$$

$$+ p_i^{AS}(t) m^A \alpha_V, \quad (6)$$

$$p_i^{RAV}(t+1) = p_i^{US}(t) (1 - r_i(t)) m^A + p_i^{RAS}(t) m^A (1 - \alpha_V) + p_i^{AS}(t) m^A (1 - \alpha_V) + p_i^{A^+V}(t) + p_i^{RAV}(t), \quad (7)$$

$$p_i^{RUV}(t+1) = p_i^{US}(t) r_i(t) m^U (1 - \alpha_V) + p_i^{RUV}(t), \quad (8)$$

$$p_i^{RAI}(t+1) = p_i^{US}(t) (1 - r_i(t)) (1 - m^A) \times (1 - q_i(t)) + p_i^{AS}(t) \times (1 - m^A) (1 - q_i(t)) + p_i^{RAS}(t) \times (1 - m^A) (1 - q_i(t)), \quad (9)$$

$$p_i^{RUI}(t+1) = p_i^{US}(t) r_i(t) (1 - m^U) (1 - q_i(t)), \quad (10)$$

$$p_i^{RAR}(t+1) = p_i^{RAI}(t) + p_i^{RAR}(t), \quad (11)$$

and

$$p_i^{RUR}(t+1) = p_i^{RUI}(t) + p_i^{RUR}(t). \quad (12)$$

In the final state, i.e.,  $t \rightarrow \infty$  in Eqs. (3)–(12), there is

$$p_i^X(t+1) = p_i^X(t) = p_i^X. \quad (13)$$

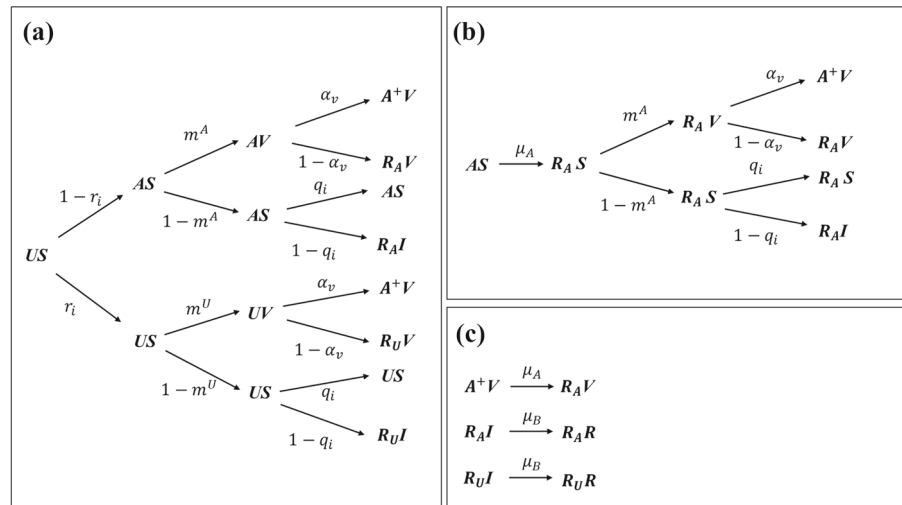
Around the epidemic threshold, the number of infected nodes is negligible compared to the total population; thus, the probability of nodes being infected can be assumed to be:  $p_i^I = p_i^{RAI} + p_i^{RUI} = \epsilon_i \ll 1$ . Equation (2) can be approximated as

$$q_i(t) = 1 - \beta_B \sum_j b_{ij} \epsilon_j = 1 - \sigma_i. \quad (14)$$

Meanwhile, since the number of infected nodes can be ignored near the critical point,  $p_i^{RAR} \rightarrow 0$  and  $p_i^{RUR} \rightarrow 0$ . Equations (3)–(8) can be written as

$$p_i^{US}(t+1) = p_i^{US}(t) r_i(t) (1 - m^U), \quad (15)$$

**Fig. 2** Transition probability trees for some states. **a** The state transition probability tree of a node in  $US$  state. **b** The state transition probability tree of a node in  $AS$  state. **c** The state transition probability trees of nodes in  $A^+V$ ,  $R_A I$ , or  $R_U I$  state, respectively. For any other state being the initial state, its transition probability tree is a sub-tree of one of the demonstrated trees



$$p_i^{AS}(t+1) = p_i^{US}(t)(1-r_i(t))(1-m^A), \quad (16)$$

$$p_i^{RAS}(t+1) = p_i^{AS}(t)(1-m^A) + p_i^{RAS}(t)(1-m^A), \quad (17)$$

$$p_i^{A^+V}(t+1) = p_i^{US}(t)(1-r_i(t))m^A\alpha_v + p_i^{US}(t)r_i(t)m^U\alpha_v + p_i^{RAS}(t)m^A\alpha_v + p_i^{AS}(t)m^A\alpha_v, \quad (18)$$

$$p_i^{RAV}(t+1) = p_i^{US}(t)(1-r_i(t))m^A + p_i^{RAS}(t)m^A(1-\alpha_v) + p_i^{AS}(t)m^A(1-\alpha_v) + p_i^{A^+V}(t) + p_i^{RAV}(t), \quad (19)$$

and

$$p_i^{RUV}(t+1) = p_i^{US}(t)r_i(t)g(1-\alpha_v) + p_i^{RUV}(t). \quad (20)$$

By summing up Eqs. (9) and (10), we get

$$\epsilon_i = p_i^{US}(1-r_i)(1-m^A)\sigma_i + p_i^{AS}(1-m^A)\sigma_i + p_i^{RAS}(1-m^A)\sigma_i + p_i^{US}r_i(1-m^U)\sigma_i. \quad (21)$$

Then, substituting Eqs. (15)–(17) into Eq. (21), we have

$$\epsilon_i = p_i^{AS}\sigma_i + p_i^{RAS}\sigma_i + p_i^{US}\sigma_i = (p_i^{AS} + p_i^{RAS} + p_i^{US})\sigma_i. \quad (22)$$

Near the threshold, we have

$$p_i^{US} + p_i^{AS} + p_i^{RAS} + p_i^{A^+V} + p_i^{RAV} + p_i^{RUV} = 1. \quad (23)$$

Since

$$p_i^{A^+V} + p_i^{RAV} + p_i^{RUV} = p_i^V, \quad (24)$$

substituting Eqs. (23) and (24) into Eq. (22), we can get

$$\epsilon_i = (p_i^{AS} + p_i^{RAS} + p_i^{US})\sigma_i = (1-p_i^V)\sigma_i = (1-p_i^V)\beta_B \sum_j b_{ij}\epsilon_j. \quad (25)$$

Equation (25) can be written in the format of matrix as

$$\sum_j \left\{ (1-p_i^V)b_{ij} - \frac{1}{\beta_B}\theta_{ij} \right\} \epsilon_j = 0, \quad (26)$$

where  $\theta_{ij}$  is the element of identity matrix. The epidemic threshold  $\beta_B^c$  is the minimum value that satisfies Eq. (25). As a self-consistent equation, obtaining  $\beta_B^c$  reduces to the eigenvalue problem for the matrix  $H$ , where the elements of  $H$  are

$$h_{ij} = (1-p_i^V)b_{ij}. \quad (27)$$

Let  $\Lambda_{\max}(H)$  be the largest eigenvalue of matrix  $H$ , the epidemic threshold is given by

$$\beta_B^c = \frac{1}{\Lambda_{\max}(H)}, \quad (28)$$

which indicates that the epidemic threshold depends on the adjacency matrix  $b_{ij}$  and the probability  $p_i^V$  of node  $i$  in  $V$  state. In calculating  $h_{ij}$ , we iterate Eqs. (15)–(20) to get  $p_i^V$  in the final state.



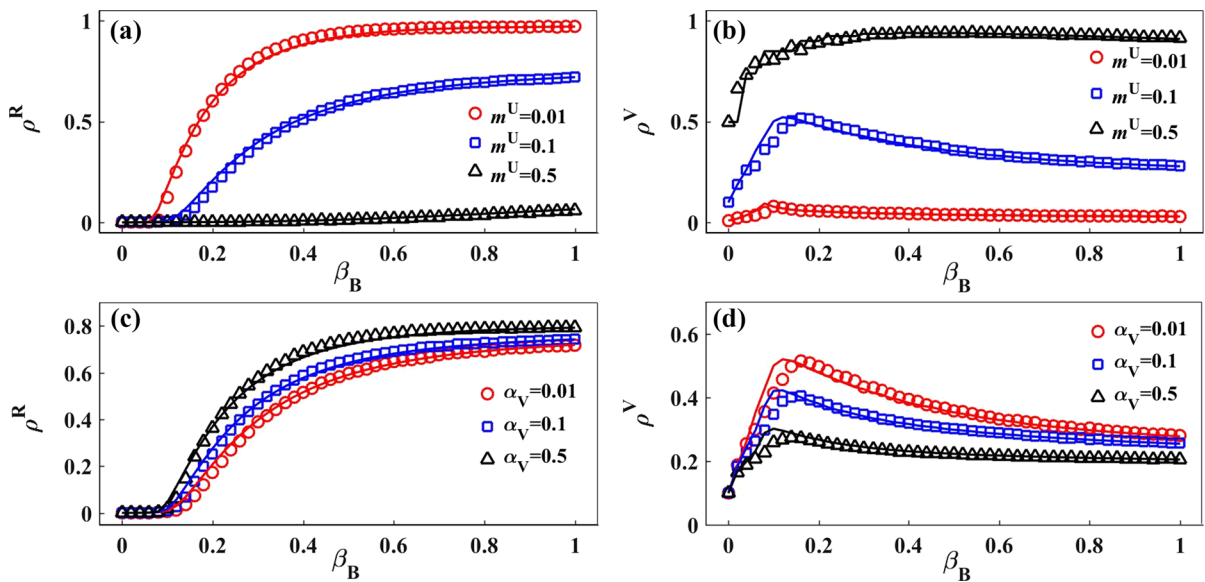


**Fig. 3** The density of removed nodes  $\rho^R$  and vaccinated nodes  $\rho^V$  as a function of disease transmission rate  $\beta_B$  obtained by the MMCA (lines) and Monte Carlo simulations (shapes). The density of removed nodes  $\rho^R$  (a) and density of vaccinated nodes  $\rho^V$  (b) at different vaccination rates  $m^U$ . When the basic vaccination rate  $m^U = 0.5$ , the disease hardly breaks out and  $\rho^R$  is small. When  $m^U = 0.01$  and  $m^U = 0.1$ , the density of vaccinated nodes increases first and then decreases. This is because below the epi-

demic threshold, the existence time of epidemic is prolonged as  $\beta_B$  increases, so the  $\rho^V$  increases with  $\beta_B$  first. Other parameters are set as  $\beta_A = 0.3$ ,  $\beta_A^+ = 0.6$ ,  $\gamma = 0$ ,  $\alpha_V = 0.01$ . The density of removed nodes  $\rho^R$  (c) and density of vaccinated nodes  $\rho^V$  (d) at different adverse event probabilities  $\alpha_V$ . With the increase of adverse event occurrence,  $\rho^R$  increases and  $\rho^V$  decreases. Other parameters are set as  $\beta_A = 0.3$ ,  $\beta_A^+ = 0.6$ ,  $\gamma = 0$ ,  $m^U = 0.1$

#### 4 Numerical simulations

We carry out extensive numerical simulations to analyze the impact of negative information diffusion on epidemic spreading. In our simulations, each layer of the multiplex network is generated from the uncorrelated configuration model (UCM), which follows a power law degree distribution [36]. The number of nodes is  $N = 10000$ , the degree distribution exponent is  $s = 2.5$ , and the minimal and maximal degrees are  $k_{min} = 5$  and  $k_{max} = N^{\frac{1}{(s-1)}}$ , respectively. The nodes of two layers are randomly connected by one-to-one interlayer links, so each node in one layer has a counterpart in the other layer. Initially, 0.1% of nodes are randomly chosen as infected seeds (i.e., being in  $R_U I$  state), 0.1% of nodes are randomly chosen as aware seeds (i.e., being in  $AS$  state), and all other nodes are in  $US$  state. For simplicity and without loss of generality, we set  $\mu_A = \mu_B = 1$ .

Firstly, we demonstrate the density of removed nodes  $\rho^R$  and vaccinated nodes  $\rho^V$  in the final

state as a function of disease transmission rate  $\beta_B$ , where  $\rho^R = \frac{1}{N} \sum_i (p_i^{R_A R} + p_i^{R_U R})$  and  $\rho^V = \frac{1}{N} \sum_i (p_i^{A^+ V} + p_i^{R_A V} + p_i^{R_U V})$ . In Fig. 3a and b, the results under different vaccination rates are compared. When the disease transmission rate  $\beta_B$  is above the outbreak threshold,  $\rho^R$  increases as  $\beta_B$  increases. A larger  $m^U$  indicates a stronger vaccination rate, which results in a smaller  $\rho^R$ . When the vaccination rate  $m^U = 0.5$ , which is very large, the disease hardly breaks out and the  $\rho^R$  is very low. As for the vaccination density  $\rho^V$ , it first increases and then decreases with disease transmission rate  $\beta_B$ . This is because below the epidemic threshold  $\beta_B^c$ , although the disease does not break out, the existence time of infected nodes in the system is prolonged as  $\beta_B$  increases. Since at each time step nodes get vaccinated at rate  $m^U$ , a longer existence time of infected nodes will result in more vaccinated nodes. When  $\beta_B$  increases above the epidemic threshold, the  $\rho^V$  decreases with  $\beta_B$  because the number of infected nodes increases. In Fig. 3c and d, results under three adverse events probability  $\alpha_V$  are compared. It can be

seen that a larger adverse events probability  $\alpha_V$  results in a higher  $\rho^R$  and a lower  $\rho^V$ . It is worth noticing that the density of removed nodes  $\rho^R$  does not increase significantly as  $\alpha_V$  increases. This is because the occurrence of adverse events only increases the number of the source nodes of negative information, while its impacts on epidemic spreading also depend on other factors, such as the negative information transmission rate  $\beta_A$ , the vaccination attenuation factor  $\gamma$  and the vaccination rate  $m^U$ . The results shown in Fig. 3 demonstrate the consistency between the theoretical predictions and the simulation results.

#### 4.1 Impact of negative information on epidemic threshold

According to the MMCA method, the epidemic threshold is determined by the matrix  $H$ , whose elements are  $h_{ij} = (1 - p_i^V) b_{ij}$ . Here  $p_i^V$  is the probability that node  $i$  is in vaccinated state. Besides the vaccination rate  $m^U$  and the adverse events probability  $\alpha_V$ , which have been discussed above, there are three parameters that may impact  $p_i^V$ : the information dissemination rate  $\beta_A$ , the transmission enhancement coefficient  $c$  and the vaccination attenuation factor  $\gamma$ . Figure 4 displays the impact of these three factors on the epidemic threshold. Both theoretical predictions and numerical simulation results are demonstrated.

The simulated epidemic threshold is obtained by using the method called susceptibility [35], where a quantity  $\chi$  is defined as:

$$\chi = \sqrt{\frac{\langle \rho^2 \rangle - \langle \rho \rangle^2}{\langle \rho \rangle}}. \quad (29)$$

In the equation,  $\rho$  is the density of removed nodes in the final state in one run, and  $\langle \rho \rangle$  is the average  $\rho$  over several runs. We implement 200 runs under each of the disease transmission rate to get a  $\chi$ , and the disease transmission rate that corresponds to the largest  $\chi$  is identified as the simulated epidemic threshold.

In Fig. 4a, it can be seen that with the increase of information transmission rate  $\beta_A$ , the epidemic outbreak threshold decreases. The wide spread of negative information makes more individuals reduce their vaccination probability, thus leading to a reduced epidemic threshold. Particularly, when  $\beta_A < 0.25$ , the theoretical threshold is much larger than the simulated

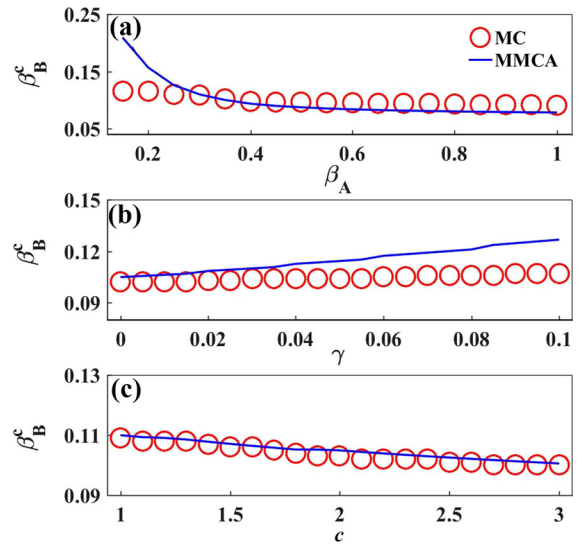


**Fig. 4** The impact of negative information on epidemic threshold  $\beta_B^c$ . **a** The epidemic threshold decreases with the information dissemination rate  $\beta_A$ . Other parameters are set as  $c = 1$ ,  $\gamma = 0$ ,  $m^U = 0.1$ ,  $\alpha_V = 0.1$ . **b** The epidemic threshold increases with the vaccination attenuation factor  $\gamma$ . Other parameters are set as  $c = 2$ ,  $\beta_A = 0.3$ ,  $m^U = 0.1$ ,  $\alpha_V = 0.1$ . **c** The epidemic threshold decreases with the transmission enhancement coefficient  $c$ . Other parameters are set as  $\beta_A = 0.3$ ,  $\gamma = 0$ ,  $m^U = 0.1$ ,  $\alpha_V = 0.1$ . Shapes are Monte Carlo (MC) simulation results, and lines are analytical results predicted by MMCA

threshold. This is because in calculating the theoretical threshold by MMCA method, the vaccination and epidemic processes are treated successively and separately. This makes the vaccination coverage larger than its size in simulations, and the epidemic is more difficult to break out [36]. When  $\beta_A > 0.25$ , the dissemination of negative information becomes large. This makes more individuals reduce their vaccination probability and prevents the theoretical vaccination coverage from being too large. In Fig. 4b, with the increase in vaccination attenuation factor  $\gamma$ , the individuals are less impacted by the negative information. Thus, the epidemic threshold increases with  $\gamma$ . The simulated epidemic threshold increases more slightly than the theoretical epidemic threshold. In Fig. 4c, as the information enhancement coefficient  $c$  increases, the dissemination rate of negative information increases ( $\beta_A^+ = c\beta_A$ ). There are more nodes affected by the negative information, and thus, the epidemic threshold decreases.



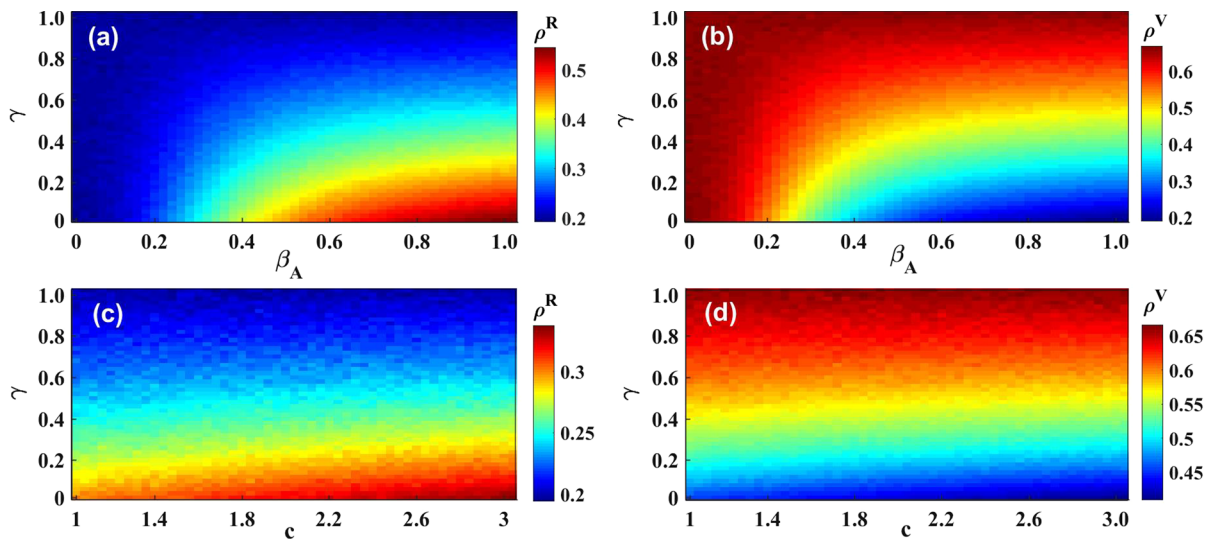


**Fig. 5** The phase diagrams of the density of removed nodes  $\rho^R$  and vaccinated nodes  $\rho^V$ . In **a** and **b**, the effects of information transmission rate  $\beta_A$  and vaccination attenuation factor  $\gamma$  are shown. When  $\beta_A$  is large enough,  $\rho^R$  decreases and  $\rho^V$  increases with  $\gamma$ . Other parameters are set as  $m^U = 0.1$ ,  $\alpha_V = 0.1$ ,  $c = 1$

and  $\beta = 0.25$ . In **c** and **d**, the effects of transmission enhancement coefficient  $c$  and vaccination attenuation factor  $\gamma$  are displayed. As  $\gamma$  increases, the  $\rho^R$  decreases and  $\rho^V$  increases. The impact of  $c$  is relatively small. Other parameters are set as  $m^U = 0.1$ ,  $\alpha_V = 0.1$ ,  $\beta_A = 0.3$  and  $\beta = 0.25$

#### 4.2 Impact of negative information on infection and vaccination

Next we investigate on the spread of negative information on the final infection size and vaccination coverage. Figure 5a and b demonstrates the phase diagrams of the density of removed nodes  $\rho^R$  and vaccinated nodes  $\rho^V$  as a function of the information transmission rate  $\beta_A$  and vaccination attenuation factor  $\gamma$ . When  $\gamma$  is relatively small, which corresponds to the case that the aware nodes reduce their vaccination probability greatly, then with the increase of information transmission rate  $\beta_A$ , the density of removed nodes  $\rho^R$  increases and the density of vaccinated nodes  $\rho^V$  decreases. When  $\gamma$  is relatively large ( $\gamma > 0.6$ ), which corresponds to case that the aware nodes reduce the vaccination probability slightly, there is no obvious change in  $\rho^R$  and  $\rho^V$  as  $\beta_A$  increases. On the other hand, the effect of  $\gamma$  depends on  $\beta_A$ . Only when the negative information can break out in the communication layer, i.e.,  $\beta_A > \beta_A^c$ , the removed density  $\rho^R$  decreases and the vaccination density  $\rho^V$  increases as  $\gamma$  increases. Figure 5c and d shows the phase diagrams of  $\rho^R$  and  $\rho^V$  as a function of the information transmission enhancement coefficient  $c$  and vaccination attenuation factor  $\gamma$ .

It can be seen that the removed density  $\rho^R$  increases and the vaccinated density  $\rho^V$  decreases slightly as  $c$  increases. This implies that a small proportion of individuals with adverse events, who transmit information at a relatively high rate, do not impact the epidemic spreading and vaccination coverage significantly.

From Fig. 5, we find that the vaccination attenuation factor  $\gamma$  and information transmission rate  $\beta_A$  have a significant impact on epidemic spreading, especially when the information transmission rate  $\beta_A$  is large and the vaccination attenuation factor  $\gamma$  is small. In real-world scenarios, if the negative information has a weak impact on the people's willingness to vaccinate corresponding to the large  $\gamma$ , the impact of negative information is slight on epidemic spreading. However, if the negative information has a strong impact on people's willingness to vaccinate corresponding to the small  $\gamma$ , the public health authority in responsibility must take necessary measures to limit the dissemination of negative information, such as showing more scientific information about vaccines and disclosing the actual cause of adverse events. In addition, individuals who have got a vaccine adverse event should not disseminate the information on social media before getting the fact,

because the spread of negative information will impede vaccination progress.

## 5 Conclusion and discussion

The widespread dissemination of negative information on vaccine may arise vaccination hesitancy among people, which will seriously impede the vaccination progress and damage epidemic control. In this study, we propose a negative information-epidemic coupled propagation model to study the impact of negative information of vaccine on epidemic spreading and vaccination coverage. By using the microscopic Markov chain method, we analytically predict the epidemic threshold and final infection size in the system, which agree well with the simulation results. We find that the dissemination of negative information reduces the epidemic outbreak threshold and makes the final infection increase and vaccination coverage decrease. Only when the affected individuals largely reduce their vaccination probability, the negative information can impact the epidemic spreading significantly. Otherwise the information spreading has a very slight impact on the epidemic spreading. To effectively suppress epidemic, people should reduce their hesitations in vaccination, which is more effective than controlling the information spreading in the social platforms.

The development and production of vaccines require a lot of money and time; thus, vaccines are actually a kind of limited resource in a certain period of time. The distribution of vaccines is a key factor that may determine the effects of vaccination in suppressing the pandemic in large populations. Furthermore, a vaccinated individual still has a chance of being infected, depending on the efficiency of vaccines. This factor should be taken into consideration when the safety of vaccines becomes less concerned and the effectiveness is more cared about. In addition to the negative information that can impact people's willingness to vaccination, the herd mentality of vaccination may also impact the vaccination behavior of individuals. The timescales of information dissemination, epidemic spreading and vaccination are different in reality. Modeling the coevolving dynamics by taking these aspects into consideration needs further study in the future.

**Author contributions** JC was involved in methodology, software, validation, formal analysis, investigation, writing—original draft, writing—review & editing. YL provided conceptualization, methodology, formal analysis, investigation, writing—original draft, writing—review & editing, funding acquisition. JY did methodology, investigation, data curation. XD done methodology, investigation, writing—original draft. MT contributed to conceptualization, formal analysis, writing—original draft, and funding acquisition.

**Funding** This work was supported by the National Natural Science Foundation of China (Grant Nos. 61802321, 11975099), the Sichuan Science and Technology Program (No. 2020YJ0125), the Natural Science Foundation of Shanghai (Grant No. 18ZR1412200) and the Southwest Petroleum University Innovation Base (No.642).

**Data availability** The datasets generated during and/or analyzed during the current study are available in the GitHub repository. <https://github.com/kumamon520/Coevolving-spreading-dynamics-of-negative-information-and-epidemic-on-multiplex-networks.git>.

## Declarations

**Conflict of interest** The authors have no relevant financial or non-financial interests to disclose.

## References

1. Dye, C., Gay, N.: Modeling the SARS epidemic. *Science* **300**, 1884–1885 (2003)
2. Baize, S., Pannetier, D., Oestereich, L., et al.: Emergence of Zaire Ebola virus disease in Guinea. *New England J. Med.* **371**, 1418–1425 (2014)
3. Chang, S., Pierson, E., Koh, P.W., et al.: Mobility network models of COVID-19 explain inequities and inform reopening. *Nature* **589**, 82–87 (2021)
4. Anderson, R.M., May, R.M.: *Infectious Diseases of Humans: Dynamics and Control*. Oxford University Press, Oxford (1992)
5. Pastor-Satorras, R., Castellano, C., Van Mieghem, P., et al.: Epidemic processes in complex networks. *Rev. Modern Phys.* **87**, 925 (2015)
6. Funk, S., Gilad, E., Watkins, C., et al.: The spread of awareness and its impact on epidemic outbreaks. *Proc. National Acad. Sci.* **106**, 6872–6877 (2009)
7. Granell, C., Gómez, S., Arenas, A.: Dynamical interplay between awareness and epidemic spreading in multiplex networks. *Phys. Rev. Lett.* **111**, 128701 (2013)
8. Granell, C., Gómez, S., Arenas, A.: Competing spreading processes on multiplex networks: awareness and epidemics. *Phys. Rev. E* **90**, 012808 (2014)
9. Wang, W., Tang, M., Yang, H., et al.: Asymmetrically interacting spreading dynamics on complex layered networks. *Scientific Rep.* **4**, 5097 (2014)

10. Kan, J.-Q., Zhang, H.-F.: Effects of awareness diffusion and self-initiated awareness behavior on epidemic spreading - An approach based on multiplex networks. *Commun. Nonlinear Sci. Numer. Simul.* **44**, 193–203 (2017)
11. Xia, C., Wang, Z., Zheng, C., et al.: A new coupled disease-awareness spreading model with mass media on multiplex networks. *Inform. Sci.* **471**, 185–200 (2019)
12. Wang, H., Ma, C., Chen, H.-S., et al.: Effects of asymptomatic infection and self-initiated awareness on the coupled disease-awareness dynamics in multiplex networks. *Appl. Math. Comput.* **400**, 126084 (2021)
13. Wang, W., Liu, Q.-H., Cai, S.-M., et al.: Suppressing disease spreading by using information diffusion on multiplex networks. *Scientific Rep.* **6**, 29259 (2016)
14. da Silva, P.C.V., Velásquez-Rojas, F., Connaughton, C., et al.: Epidemic spreading with awareness and different timescales in multiplex networks. *Phys. Rev. E* **100**, 032313 (2019)
15. Velásquez-Rojas, F., Ventura, P.C., Connaughton, C., et al.: Disease and information spreading at different speeds in multiplex networks. *Phys. Rev. E* **102**, 022312 (2020)
16. Guo, Q., Jiang, X., Lei, Y., et al.: Two-stage effects of awareness cascade on epidemic spreading in multiplex networks. *Phys. Rev. E* **91**, 012822 (2015)
17. Wang, Z., Guo, Q., Sun, S., et al.: The impact of awareness diffusion on SIR-like epidemics in multiplex networks. *Appl. Math. Comput.* **349**, 134–147 (2019)
18. Wang, H., Chen, C., Qu, B., et al.: Epidemic mitigation via awareness propagation in communication networks: the role of time scales. *New J. Phys.* **19**, 073039 (2017)
19. Wang, Z., Xia, C., Chen, Z., et al.: Epidemic propagation with positive and negative preventive information in multiplex networks. *IEEE Trans. Cybern.* **51**, 1454–1462 (2020)
20. Wang, X., Zhu, X., Tao, X., et al.: Anomalous role of information diffusion in epidemic spreading. *Phys. Rev. Res.* **3**, 013157 (2021)
21. Paré, P.E., Liu, J., Beck, C.L., et al.: Multi-competitive viruses over time-varying networks with mutations and human awareness. *Automatica* **123**, 109330 (2021)
22. Chou, W.-Y.S., Oh, A., Klein, W.M.P.: Addressing health-related misinformation on social media. *Jama* **320**, 2417–2418 (2018)
23. Scheufele, D.A., Krause, N.M.: Science audiences, misinformation, and fake news. *Proc. National Acad. Sci.* **116**, 7662–7669 (2019)
24. Gallotti, R., Valle, F., Castaldo, N., et al.: Assessing the risks of ‘infodemics’ in response to COVID-19 epidemics. *Nature Human Behaviour* **4**, 1285–1293 (2020)
25. Pulido, C.M., Villarejo-Carballido, B., Redondo-Sama, G., et al.: COVID-19 infodemic: More retweets for science-based information on coronavirus than for false information. *Int. Sociol.* **35**, 377–392 (2020)
26. De Figueiredo, A., Simas, C., Karafillakis, E., et al.: Mapping global trends in vaccine confidence and investigating barriers to vaccine uptake: a large-scale retrospective temporal modelling study. *The Lancet* **396**, 898–908 (2020)
27. Spier, R.E.: Perception of risk of vaccine adverse events: a historical perspective. *Vaccine* **20**, 78–84 (2001)
28. Guimaraes, L.E., Baker, B., Perricone, C., et al.: Vaccines, adjuvants and autoimmunity. *Pharmacol. Res.* **100**, 190–209 (2015)
29. Loomba, S., de Figueiredo, A., Piatek, S.J., et al.: Measuring the impact of COVID-19 vaccine misinformation on vaccination intent in the UK and USA. *Nature Human Behaviour* **5**, 337–348 (2021)
30. Bhattacharyya, S., Vutha, A., Bauch, C.T.: The impact of rare but severe vaccine adverse events on behaviour-disease dynamics: a network model. *Scientific Rep.* **9**, 7164 (2019)
31. Sharevski, F., Alsaadi, R., Jachim, P., et al.: Misinformation warning labels: Twitter’s soft moderation effects on COVID-19 vaccine belief echoes. [arXiv:2104.00779v1](https://arxiv.org/abs/2104.00779v1) (2021)
32. Muric, G., Wu, Y., Ferrara, E.: COVID-19 vaccine hesitancy on social media: building a public twitter dataset of anti-vaccine content, vaccine misinformation and conspiracies. *JMIR Public Health Surveill* **7**, e30642 (2021)
33. Yin, Q., Wang, Z., Xia, C., et al.: Impact of co-evolution of negative vaccine-related information, vaccination behavior and epidemic spreading in multilayer networks. *Commun. Nonlinear Sci. Numer. Simul.* **109**, 106312 (2022)
34. Zhang, J., Litvinova, M., Liang, Y., et al.: Changes in contact patterns shape the dynamics of the COVID-19 outbreak in China. *Science* **368**, 1481–1486 (2020)
35. Ferreira, S.C., Castellano, C., Pastor-Satorras, R.: Epidemic thresholds of the susceptible-infected-susceptible model on networks: A comparison of numerical and theoretical results. *Phys. Rev. E* **86**, 041125 (2012)
36. Newman, M.E.J.: Threshold effects for two pathogens spreading on a network. *Phys. Rev. Lett.* **95**, 108701 (2005)

**Publisher’s Note** Springer Nature remains neutral with regard to jurisdictional claims in published maps and institutional affiliations.

Springer Nature or its licensor holds exclusive rights to this article under a publishing agreement with the author(s) or other rightsholder(s); author self-archiving of the accepted manuscript version of this article is solely governed by the terms of such publishing agreement and applicable law.